NIH Public Access
Author Manuscript
Anal Chem. Author manuscript; available in PMC 2011 April 1.

Published in final edited form as:
Anal Chem. 2010 April 1; 82(7): 3061–3066. doi:10.1021/ac100251d.

Surface Fragmentation of Complexes from Thiolate Protected Gold Nanoparticles by Ion Mobility-Mass Spectrometry

Kellen M. Harkness, **Larissa S. Fenn**, **David E. Cliffel**, and **John A. McLean**
Department of Chemistry, Vanderbilt Institute of Chemical Biology, Vanderbilt Institute for Integrative Biosystems Research and Education, Vanderbilt University, 7330 Stevenson Center, Nashville, TN 37235, USA

Abstract

Matrix-assisted laser desorption/ionization-ion mobility-mass spectrometry (MALDI-IM-MS) was used to analyze low mass gold-thiolate fragments generated from thiolate-protected gold nanoparticles (AuNPs). This is the first report of using gas-phase structural separations by IM-MS for the characterization of AuNPs, revealing significant structural variation between organic and gold-thiolate ionic species. Through the separation of background chemical noise, gold-thiolate ion species corresponding to fragments from the AuNP surface can be isolated. In the negative ion mode, many of these fragments correlate to capping structural motifs observed in the literature. In the positive ion mode, the fragment ions do not correlate to predicted structural motifs, but are nearly identical to the positive ions generated from the gold-thiolate AuNP precursor complexes. This suggests that energetic processes during laser desorption/ionization induce a structural rearrangement in the capping gold-thiolate structure of the AuNP, resulting in the generation of positively charged gold-thiolate complexes similar to the precursors of AuNP formation by reduction and negatively charged complexes more representative of the AuNP surface.

INTRODUCTION

Thiolate-protected gold nanoparticles (AuNPs) are a versatile nanomaterial with an expanding array of applications ranging from biomimicry[1] to molecular electronics.2 Full characterization of any ligand-protected AuNP, *i.e.*, non-averaging measurement of size and molecular composition, is not currently possible in a single analytical platform. Mass spectrometry (MS) has shown considerable promise as a characterization technique, whereby gold cores less than 2 nm in diameter have been sized by MS,[3] and intact AuNP analysis is theoretically capable of providing both size and molecular composition information.4 However, AuNP characterization by MS is currently effective only for hydrophobic ligand-protected AuNPs up to *ca.* 2 nm in diameter[5] and hydrophilic AuNPs with 39 gold atoms or less (*ca.* 1.1 nm in diameter).[6] Nevertheless, past work has proven that MS is capable of revealing information about AuNPs which is otherwise difficult, if not impossible, to obtain otherwise.

In 2007, Cliffel and colleagues studied tiopronin (Tio)-protected AuNPs by electrospray (ESI)-MS and discovered a tetrameric $Au_4(Tio)_4$ ion, which was putatively assigned to be an 8-membered ring.[7] This assignment was based on the "divide and protect" capping motif proposed by Häkkinen *et al.*, in which 8-membered, tetrameric $Au_4(SCH_3)_4$ rings were predicted to protect the core of the $Au_{38}(SCH_3)_{24}$ nanoparticle.[8] This first experimental hint of discrete gold-thiolate structural motifs on the surface of AuNPs was dramatically reinforced by Kornberg and coworkers' 2007 crystal structure of Au_{102}(*p*-MBA)$_{44}$, which revealed semi-

d.cliffel@vanderbilt.edu; john.a.mclean@vanderbilt.edu.

NIH-PA Author Manuscript
NIH-PA Author Manuscript
NIH-PA Author Manuscript

NIH-PA Author Manuscript

NIH-PA Author Manuscript

NIH-PA Author Manuscript

ring "staple" capping structures.[9] In the first unfragmented MALDI spectrum of an AuNP, that of $[Au_{25}(SCH_2CH_2Ph)_{18}]^+$, a fragment corresponding to a loss of $Au_4(SCH_2CH_2Ph)_4$ appeared at increased laser fluence.[4] This loss has also been observed from $Au_{38}(SCH_2CH_2Ph)_{24}$ and $Au_{68}(SCH_2CH_2Ph)_{34}$ nanoparticles.[10] Murray and coworkers later published the crystal structure of $[Au_{25}(SCH_2CH_2Ph)_{18}]^-$,[11] in which no $Au_4(SCH_2CH_2Ph)_4$ features were observed. In the crystal structure, the nanoparticle was negatively charged, with a tetraoctylammonium counterion; in the mass spectrum, the $Au_4(SCH_2CH_2Ph)_4$ loss was the most prominent fragment ion in positive mode. Investigation of low-mass AuNP fragments (<2000 m/z), such as the $Au_4(SR)_4$ ion, would likely yield a greater understanding of the capping structural motifs of AuNPs. However, significant chemical noise can create a continuous background signal which obscures diagnostically important signals.

A complementary technique which has been used for the analysis of ligand-protected AuNPs in the gas-phase is ion mobility spectrometry (IMS). The physical property providing separation selectivity in IMS is ion size, specifically ion surface area. Briefly, in IMS ions are injected into a gas-filled drift tube where they experience numerous low-energy collisions with a background gas which separates ions based on the ion-neutral collision cross section (CCS). Smaller ions elute faster than larger ions which experience more collisions. IMS was used for measuring the diameter of ligand-protected AuNPs,[12] but the majority of IMS work relevant to this report has focused on small gold clusters generated from gold surfaces. Following the work of Jarrold *et al.*,[13,14] in 2002 Kappes and colleagues published two reports on positively[15] and negatively[16] charged gold clusters (< 25 atoms). The ion CCS of each cluster yielded a determination of their respective geometries. The ability to distinguish between various three-dimensional geometries for very small gold clusters illustrates the structural capabilities of IMS for small inorganic clusters.

Building on this foundation, we report the first application of combined ion mobility-mass spectrometry (IM-MS) to the analysis of ligand-protected AuNPs. By integrating mass and ion CCS separation, gold-thiolate ions can be isolated from nearly isobaric but larger organic ions (*i.e.*, chemical noise). Furthermore, the structural measurement capabilities of IM-MS, which have been well-documented for biomolecules,[17] could theoretically be applied in order to obtain an unprecedented amount of structural information from these ions. Because of the two advantages of signal-to-noise enhancement and structural characterization capability, IM-MS is well-suited for the study of low-mass fragments generated from ligand-protected AuNPs. The samples used in this work consisted of AuNPs protected by tiopronin or phenylethanethiolate as well as gold-tiopronin and gold-phenylethanethiolate precursor complexes for comparison using MALDI-IM-MS.

EXPERIMENTAL SECTION

Tiopronin- and phenylethanethiolate-protected AuNPs were synthesized using previously reported protocols.[7,18] The tiopronin-protected AuNPs were found to be 3.0 ± 0.8 nm in diameter by transmission electron microscopy. Gold-tiopronin and gold-phenylethanethiolate precursor complexes were formed by combining tetrachloroauric acid with 3 molar equivalents of tiopronin ([(2-mercaptopropanoyl)amino]acetic acid, Sigma-Aldrich) and phenylethanethiol (98%, Aldrich) respectively in dry methanol (Fisher) at 0° C. The gold-phenylethanethiolate complex aggregated immediately and became insoluble, creating a slurry; gold-tiopronin created a cloudy solution. After 30 min., 100 μL aliquots of the gold-tiopronin solution and gold-phenylethanethiolate complex slurry were collected.

Samples were prepared for MALDI analysis by the dried droplet method.[19] The samples were combined with matrix in solution and 0.5 – 1.5 μL of the sample was deposited on a stainless

NIH-PA Author Manuscript

NIH-PA Author Manuscript

NIH-PA Author Manuscript

steel plate. Tiopronin-protected AuNPs were saturated in 50 μL of deionized H_2O and combined with 50 μL of dry methanol. Each sample was combined with 30 mg α-cyano-4-hydroxycinnamic acid (Sigma), and 1 mg sodium chloride (certified A.C.S., Fisher) was added to all samples except for the gold-phenylethanethiolate in order to obtain better signal from sodium-coordinated species. To a 3 mg sample of phenylethanethiol-protected AuNPs was added 100 μL acetone (Fisher) and combined with 30 mg *trans*-2-[3-(4-*tert*-butyl-phenyl)-2-methyl-2-propenylidene]malononitrile (DCTB, Fluka).[4] Each mixture was sonicated immediately prior to spotting on the MALDI plate.

All spectra were obtained on a Synapt HDMS ion mobility-mass spectrometer (Waters Corp., Manchester, UK) equipped with a MALDI ion source. A travelling wave (T-wave)-ion mobility cell[20] was utilized for ion mobility separation in nitrogen gas. The ion guide T-wave was operated at 300 m s^{-1} and linearly ramped in amplitudes ranging from 1-17 V to 5-20 V for each experiment. The transfer guide T-wave was operated at 248 m s^{-1} with a constant 3 V amplitude. Trap and transfer ion injection voltages were set at 6 and 4 V, respectively. MassLynx 4.1 software (Waters Corp., Milford, MA) was used for instrument control and data processing.

RESULTS AND DISCUSSION

Figure 1A is an illustration of a typical two-dimensional IM-MS spectrum, in which the abscissa axis is m/z and the ordinate axis represents drift time, which correlates to CCS. The plot can be viewed as a density map, with the upper-left quadrant being low mass and high drift time, or effectively low density. The lower right quadrant contains ions of high mass and low drift time, thus having a relatively high density. Chemical noise, composed of extensively fragmented and adducted organic ions, is present in a band of roughly constant density that spans from the lower left quadrant to the upper right. Incorporation of a gold atom within the ion increases the mass by 197 Da while increasing the CCS by a small amount. This effect creates an ion mobility shift to regions of higher density, similar to the effect of covalently bound ion mobility shift reagents utilized by McLean and co-workers.[21,22] Greater numbers of gold atoms in the ion impart a corresponding increase in density. The cumulative pattern of gold-thiolate ions in ion mobility-mass spectrometry is the presence of multiple bands which are nearly parallel. Each band, counting from left to right, corresponds to the number of gold atoms present in the ions of that band. Within a given band, ions with a greater number of bound ligands will show up higher in the band, while ions with fewer will show up at the bottom of the band. These gold-thiolate ion trendlines are slightly inflected with respect to the organic ion trendline. A higher organic content dilutes the increased density effect and brings the overall density closer to that of the organic ion trend.

Figure 1B is a two-dimensional IM-MS plot from tiopronin-protected AuNPs. The gold-thiolate ion species are gold-thiolate complexes, in which the gold and sulfur atoms have formal charges of +1 and −1, respectively, although the gold-sulfur bonds have a covalent character and the electrons are delocalized throughout the gold-sulfur sequence. These ions are products of dissociation from the AuNP surface. The negative ions observed in Figure 1B are products of carboxylic acid deprotonation or C-S thiolate bond cleavage. Methyl esterified ions are also present as M+14 peaks. The methyl esterification is present due the high concentration of methanol and acid during synthesis. The lower portion of each band is generally composed of ions with fragmented ligands, most of which are products of thiolate C-S bond cleavage. A wide range of gold/tiopronin stoichiometries can be observed, including ions with much larger numbers of gold atoms than thiolate ligands (*e.g.*, $Au_{13}(Tio)_8$); however, the majority of ions observed contain an equal amount of gold and ligands, $Au_x(Tio)_x$, one less gold than ligands, $Au_x(Tio)_{x+1}$, or one more gold atom than ligands, $Au_{x+1}(Tio)_x$. As in previously reported work,[23] these structures have charges of 0, −1, and +1, respectively.

NIH-PA Author Manuscript

NIH-PA Author Manuscript

NIH-PA Author Manuscript

It is reasonable to assume that the $Au_x(Tio)_x$ species is cyclical in light of other experimental[24] and computational[25] work; the strong preference of these species for x = 4 suggests a discrete, closed structure. Cycles are known structures for gold-thiolate complexes; [26] among these cycles, tetramers are somewhat favored.[25,27,28] The $Au_x(Tio)_{x+1}$ ions correspond to the semi-ring "staple" capping structures which have been intensively studied in recent years.[29-31] The structure of the $Au_{x+1}(Tio)_x$ species is not as clear, but is likely influenced by the same types of structures previously found for the first two motifs. For the sake of clarity, these species will be referred to as linear since gold-thiolate complexes are known to form linear, open chain structures.[26]

In Figure 1B, the most notably absent ion species are staple $Au_x(Tio)_{x+1}$ ions where x > 3. This reflects the desorption of staple capping motifs from the AuNP surface, which are known to exist in x = 1,2 states crystallographically.[9,11] The presence of an x = 3 ion species may be evidence of the existence of longer staples in tiopronin-capped AuNPs. In comparison, the largest $Au_x(Tio)_x$ and $Au_{x+1}(Tio)_x$ species (including ions with ligand fragmentation) have x = 8 and 9, respectively. These larger ions are much more likely to have ligand fragmentation; the largest cyclical and linear ion species with unfragmented ligands are $Au_6(Tio)_6$ and $Au_5(Tio)_4$, respectively.

Figure 2A is a two-dimensional plot of positive ions generated from tiopronin-protected AuNPs. The utility of separating chemical noise by IM-MS is illustrated by the signal-to-noise enhancement shown in Figure 2B and 2C. Fig. 2B shows the mass spectrum integrating signals over all IM-MS conformation space, *i.e.*, what would be obtained without IM separation. Only the high intensity $Au_4(Tio)_4$ ion species are visible, but through IM separation, signals can be extracted from the gold-thiolate ion region as outlined in Fig. 2A. Note that noise is greatly reduced and low intensity signals can be observed, as shown in Fig. 2C. Clearly, low intensity signals corresponding to other cyclical, linear, and staple species would not be observed in the presence of the continuous chemical noise background. In comparison with the negative ion mode spectrum, the preference for the cyclical ion is much stronger. The $[Au_4(Tio)_4+Na]^+$ ion is the most abundant among the gold-thiolate ion species.[4,10] The $Au_2(Tio)_3$ and $Au_3(Tio)_4$ ion species are present in very low abundance, and are the only $Au_x(Tio)_{x+1}$ ion species observed. Since the $Au_x(SR)_{x+1}$ species correspond to the only capping motif which has been proven to date, their presence in a mass spectrum generated from AuNPs is not unexpected. There is evidence in the literature that capping structures can be directly desorbed from the AuNP surface: the crystallographically demonstrated $Au_2(SR)_3$ staples of the $Au_{25}(SR)_{18}$ cluster have been observed by ESI-MS/MS.[23]

Given that capping motifs can be desorbed from the AuNP surface, the dominance of the tetrameric cycle in these spectra raises the possibility of a capping motif different from the RS-$(AuSR)_x$ complex. In the literature, the tetrameric $Au_4(SR)_4$ can be found as a neutral loss from small AuNPs.[4,10] The observation of abundant $[Au_{21}(SCH_2CH_2Ph)_{14}]^+$, $[Au_{34}(SCH_2CH_2Ph)_{20}]^+$, and $[Au_{64}(SCH_2CH_2Ph)_{30}]^+$ ions,[10] each reflecting this loss, suggests that the elimination of the tetramer may be driven by a common dissociation pathway. The natively neutral tetramer can also be observed as an ion through coordination to sodium, as revealed in recent tandem MS spectra of the $Au_{25}(SR)_{18}$ cluster.[23] Since the structure of this cluster is known,[11,32] the authors noted that the $Au_4(SR)_4$ motif is not seen in the crystal structure of this cluster. This implied that rearrangement may occur within the cluster prior to fragmentation. Since the tetramer was observed as a product of rearrangement for phenylethanethiolate-protected AuNP mass spectra obtained using an ESI source with collision-induced dissociation, we next explored the extent of rearrangement present in the phenylethanethiolate-protected AuNP MALDI spectra.

NIH-PA Author Manuscript

NIH-PA Author Manuscript

NIH-PA Author Manuscript

Results of the analyses of the structurally characterized $Au_{25}(SCH_2CH_2Ph)_{18}$ cluster using MALDI-IM-MS are shown in Figure 3. The most prominent peaks correspond to linear $Au_{x+1}(SCH_2CH_2Ph)_x$ ion species, the $[Au_4(SCH_2CH_2Ph)_4]^+$ ion, and a low-abundance $Au_2(SCH_2CH_2Ph)_3$ staple ion species. Since previous ESI and MALDI spectra show the loss of the tetramer as a neutral, the $[Au_4(SCH_2CH_2Ph)_4]^{+\cdot}$ ion abundance in Figure 3 may be small compared to the amount of tetramer lost as a neutral. Otherwise, the abundances of the ions appear to correspond to the efficiency of cationization, *i.e.*, the natively positive linear ion species are high in abundance, while the cyclic and anionic staples are lower in abundance. Thus the types and abundances of the ions generated from $Au_{25}(SCH_2CH_2Ph)_{18}$ do not reflect only the crystallographically observed structural components of the cluster,[11] implying potential rearrangements during the fragmentation process. It is likely that other AuNPs also undergo such rearrangements during ionization.

Another aspect of IM-MS is the ability to characterize both gold-thiolate precursor complexes and the corresponding AuNPs in positive and negative mode, making this experimental technique a powerful method for the interactions of gold-thiolate complexes with the AuNP core. Figure 4 contains spectra generated from the gold-tiopronin precursor complex (top) and from tiopronin-protected AuNPs (bottom) in both the positive (left) and negative (right) ion modes. A careful analysis of the spectra shown in Figure 4 reveals three important patterns.

The first notable pattern observed in Figure 4 is the abundance of the $Au_x(Tio)_{x+1}$ staple ions. This pattern is significant since, as previously discussed, these ions reflect the desorption of protecting gold-thiolate complexes from the AuNP surface without rearrangement. While they are not observed in the positive ion spectrum of the gold-tiopronin precursor complex, they are present in the spectrum of the corresponding AuNPs. Furthermore, in the negative ion mode these staple ions are much more abundant from the AuNP surface than from the corresponding precursor complex. Thus, overall the staple ion species are much more abundantly generated from AuNPs than precursor complexes. This strongly implies the existence of $Au_x(Tio)_{x+1}$ capping structural motifs on the AuNP surface.

The second pattern observed in Figure 4 is the abundance of the cyclic ions. These ions are dominant, being the base peak among the gold-thiolate ions for each spectrum. The tetramer is the most abundant in the positive ion mode, in agreement with results obtained by an analogous ESI-MS experiment.[7] This agreement suggests that the dominance of the $Au_4(Tio)_4$ tetramer in the analysis of the gold-tiopronin complex is not based on sample preparation or ionization conditions, and that it is present in both in solution and in the solid phase. However, the tetramer is less dominant in the negative ion mode, particularly in the spectrum of the gold-tiopronin complex. Since smaller species are much more dominant in this spectrum, these species may be products of the fragmentation of the larger cycles into smaller species. It is important to note that, in the negative ion spectra, ionization is achieved by deprotonation or ligand C-S bond cleavage.

The final pattern concerns the conditions under which high abundances of these ions are observed. The tetrameric cycle, which appears to be the dominant form of the precursor gold-tiopronin complex, is most abundant in the positive ion mode and in the negative ion spectrum of tiopronin-protected AuNPs. The staple ion species, which correspond to capping structural motifs which have been both predicted from theory[29,30,33] and observed experimentally,[9,11,31] are also abundant in the spectra generated from AuNPs, particularly in the negative mode. Thus, it appears that negative ion products from AuNPs reflect more accurately the capping motifs of AuNPs, while positive ion products reflect a rearrangement that favors precursor-like ions. It may be significant to note that the linear ion species, which could possibly represent staple structures with the two “anchoring” gold atoms desorbed together, are more abundant in the negative ion spectrum of the AuNPs. The high abundance of the linear ion species in

NIH-PA Author Manuscript

NIH-PA Author Manuscript

NIH-PA Author Manuscript

this spectrum is particularly unexpected considering its natively positive charge. While the negative ion products largely reflect desorption with less rearrangement, the abundance of the negatively charged tetramer generated from AuNPs is noteworthy.

Given the abundance of tetrameric and larger ions observed in our studies, it is possible that larger AuNPs have larger substructures as capping motifs than the conventional 1 and 2 gold staples currently seen in the crystal structures of small AuNPs. Grönbeck *et al.* reported density functional calculations that compared a variety of capping structural motifs, including the cyclical tetramer, open linear chains, and staples with regard to their relative energies.[29] The cyclic tetramer was 0.53 eV/unit cell higher in energy than the staple capping motif, suggesting the preference for staple motifs. However, the energy difference between *cis*- and *trans*-orientations for staples with short SCH_3 ligands was calculated to be 0.69 eV/unit cell. This suggests that ligand interactions may have a substantial effect on the potential energy landscape of gold-thiolate capping motifs. While the typical ligand used for computational studies has been methanethiolate,[29-31] the hydrophilicity and hydrogen bonding availability of tiopronin should increase the degree of ligand interactions, and the corresponding effect on the gold-sulfur structures which support them.

More recent evidence supports the idea of capping structure heterogeneity. Crystal structures have been achieved for clusters with a uniform monolayer of $Au(SR)_2$ or $Au_2(SR)_3$ staples, but recent mass spectrometric reports on a larger AuNP have observed multiple molecular formulae for what was thought to be a single, discrete "magic size:" $Au_{144}(SR)_{59}$,[5] $Au_{144}(SR)_{60}$,[34,35] and $Au_{146}(SR)_{59}$.[35]. The close proximity of these assignments suggests that the difference between them may be in part from differences in the capping structural motifs. Indeed, tandem MS of the $Au_{146}(SR)_{59}$ cluster revealed a product ion corresponding to a loss of $Au_2(SR)_3$,[35] a staple structure not predicted for the $Au_{144}(SR)_{60}$ cluster.[36] In addition, the $Au_{68}(SR)_{34}$ cluster has been predicted to be formulated as $Au_{19+30}(Au(SR)_2)_{11}(Au_2(SR)_3)_4$; *i.e.*, an Au core with 11 $Au(SR)_2$ staples and 4 $Au_2(SR)_3$ staples. In light of the emerging evidence for capping structural heterogeneity, it is possible that cyclical and staple capping motifs could be present on the AuNP surface together for larger AuNPs.

CONCLUSION

We have demonstrated the capability of MALDI-IM-MS to analyze low-mass fragments generated from thiolate-protected AuNPs. This study underscores the advantages of structural separation prior to MS, and also provides a foundation for the facile characterization of thiolate-protected AuNP surfaces and gold-thiolate complexes. These surfaces are difficult to characterize using traditional experimental methods. This report highlights some of the advantages of the IM-MS approach by analyzing the product ions of thiolate-protected AuNPs and gold-thiolate complexes. We have demonstrated how the energetic ionization of AuNPs in the MALDI process produces positive fragment ions which are nearly identical to the gold-thiolate precursor complex. These similarities reveal an unexpected but rational reversal of the reduction of the precursor complex, and highlight the role of gold-thiolate complexes in the capping of AuNPs. The negative ions generated in the same process more strongly correlate to capping structural motifs that are well-established in the literature. Using this technique, we have explored capping structural motifs of larger, hydrophilic AuNPs, revealing known staple capping motifs and possible cyclical capping structures.

Acknowledgments

Financial support for this work was provided by the Vanderbilt Chemical Biology Interface (CBI) training program (T32 GM065086) in support of K.M.H., NIH GM 076479 to D.E.C., the Vanderbilt College of Arts and Sciences, the Vanderbilt Institute of Chemical Biology, the Vanderbilt Institute of Nanoscale Science and Engineering, and the Vanderbilt Institute for Integrative Biosystems Research and Education.

NIH-PA Author Manuscript

NIH-PA Author Manuscript

NIH-PA Author Manuscript

References

1. Cliffel, DE.; Turner, BN.; Huffman, BJ. In Wiley Interdisciplinary Reviews: Nanomedicine and Nanobiotechnology. James, R.; Baker, J., editors. Vol. 1. John Wiley & Sons, Inc.; Hoboken, New Jersey: 2009. p. 47-59.
2. Cervera J, Manzanares JA, Mafe S. J. Appl. Phys 2009;105:074315.
3. Schaaff TG, Shafigullin MN, Khoury JT, Vezmar I, Whetten RL, Cullen WG, First PN, Gutierrez-Wing C, Ascensio J, Jose-Yacaman MJ. J. Phys. Chem. B 1997;101:7885–7891.
4. Dass A, Stevenson A, Dubay GR, Tracy JB, Murray RW. J. Am. Chem. Soc 2008;130:5940–5946. [PubMed: 18393500]
5. Chaki NK, Negishi Y, Tsunoyama H, Shichibu Y, Tsukuda T. J. Am. Chem. Soc 2008;130:8608–8610. [PubMed: 18547044]
6. Negishi Y, Takasugi Y, Sato S, Yao H, Kimura K, Tsukuda T. J. Am. Chem. Soc 2004;126:6518–6519. [PubMed: 15161256]
7. Gies AP, Hercules DM, Gerdon AE, Cliffel DE. J. Am. Chem. Soc 2007;129:1095–1104. [PubMed: 17263390]
8. Häkkinen H, Walter M, Grönbeck H. J. Phys. Chem. B 2006;110:9927–9931. [PubMed: 16706449]
9. Jadzinsky PD, Calero G, Ackerson CJ, Bushnell DA, Kornberg RD. Science 2007;318:430–433. [PubMed: 17947577]
10. Dass A. J. Am. Chem. Soc 2009;131:11666–11667. [PubMed: 19642643]
11. Heaven MW, Dass A, White PS, Holt KM, Murray RW. J. Am. Chem. Soc 2008;130:3754–3755. [PubMed: 18321116]
12. Tsai DH, Zangmeister RA, Pease LF, Tarlov MJ, Zachariah MR. Langmuir 2008;24:8483–8490. [PubMed: 18661963]
13. Jarrold MF, Bower JE. J. Chem. Phys 1993;98:2399–2407.
14. Jarrold MF, Bower JE. J. Phys. Chem 1993;97:1746–1748.
15. Gilb S, Weis P, Furche F, Ahlrichs R, Kappes MM. J. Chem. Phys 2002;116:4094–4101.
16. Furche F, Ahlrichs R, Weis P, Jacob C, Gilb S, Bierweiler T, Kappes MM. J. Chem. Phys 2002;117:6982–6990.
17. Fenn LS, McLean JA. Anal. Bioanal. Chem 2008;391:905–909. [PubMed: 18320175]
18. Zhu M, Lanni E, Garg N, Bier ME, Jin R. J. Am. Chem. Soc 2008;130:1138–1139. [PubMed: 18183983]
19. Karas M, Hillenkamp F. Anal. Chem 1988;60:2299–2301. [PubMed: 3239801]
20. Giles K, Pringle SD, Worthington KR, Little D, Wildgoose JL, Bateman RH. Rapid Commun. Mass Spectrom 2004;18:2401–2414. [PubMed: 15386629]
21. Fenn LS, McLean JA. Chem. Commun. (Cambridge, U. K.) 2008:5505–5507.
22. Gant-Branum RL, Kerr TJ, McLean JA. Analyst 2009;134:1525–1530.
23. Fields-Zinna CA, Sampson JS, Crowe MC, Tracy JB, Parker JF, deNey AM, Muddiman DC, Murray RW. J. Am. Chem. Soc. 2009
24. Simpson, CA.; Huffman, BJ.; Harkness, KM.; Tian, P.; Billinge, SJL.; Cliffel, DE. in preparation
25. Grönbeck H, Walter M, Häkkinen H. J. Am. Chem. Soc 2006;128:10268–10275. [PubMed: 16881657]
26. Shaw CF. Chem. Rev. (Washington, DC, U. S.) 1999;99:2589–2600.
27. Bonasia PJ, Gindelberger DE, Arnold J. Inorg. Chem 1993;32:5126–5131.
28. Howard-Lock HE. Metal-Based Drugs 1999;6:201–209. [PubMed: 18475894]
29. Grönbeck H, Häkkinen H, Whetten RL. J. Phys. Chem. C 2008;112:15940–15942.
30. Jiang DE, Dai S. J. Phys. Chem. C 2009;113:7838–7842.
31. Voznyy O, Dubowski JJ, Yates JT, Maksymovych P. J. Am. Chem. Soc 2009;131:12989–12993. [PubMed: 19737018]
32. Zhu MZ, Eckenhoff WT, Pintauer T, Jin RC. J. Phys. Chem. C 2008;112:14221–14224.
33. Akola J, Walter M, Whetten RL, Hakkinen H, Gronbeck H. J. Am. Chem. Soc 2008;130:3756–3757. [PubMed: 18321117]

NIH-PA Author Manuscript

NIH-PA Author Manuscript

NIH-PA Author Manuscript

34. Qian HF, Jin RC. Nano Lett 2009;9:4083–4087. [PubMed: 19995083]
35. Fields-Zinna CA, Sardar R, Beasley CA, Murray RW. J. Am. Chem. Soc 2009;131:16266–16271. [PubMed: 19845358]
36. Lopez-Acevedo O, Akola J, Whetten RL, Gronbeck H, Hakkinen H. J. Phys. Chem. C 2009;113:5035–5038.

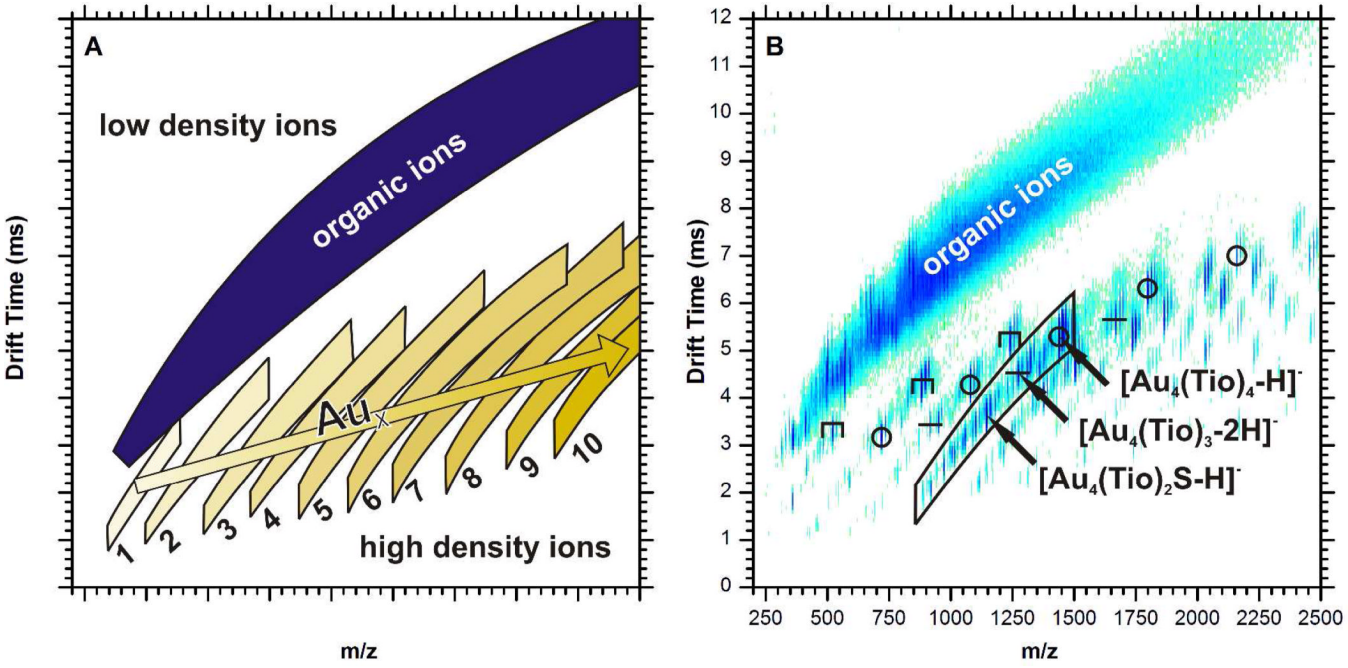

Figure 1.

An illustration of a typical ion mobility-mass spectrum of thiolate-protected AuNPs (A), where the numbers are *x* for $Au_x(SR)_y$, and an ion mobility-mass spectrum of tiopronin-protected AuNPs in negative ion mode (B). A broad band in the top-left of the spectrum is composed of organic ions. The small bands below and to the right of the major organic ion band correspond respectively to the number of gold atoms (*x*) contained in the ions of that band. Ions higher in each band correspond to species with a higher organic content, while ions lower in the bands have lower organic content, often due to fragmentation. The symbols above the ion species in the IM-MS plot indicate their assigned structure: ring (○), linear (–), and staple (Π). The placement of the ion species in the plot gives clues for structural analysis.

NIH-PA Author Manuscript
NIH-PA Author Manuscript
NIH-PA Author Manuscript

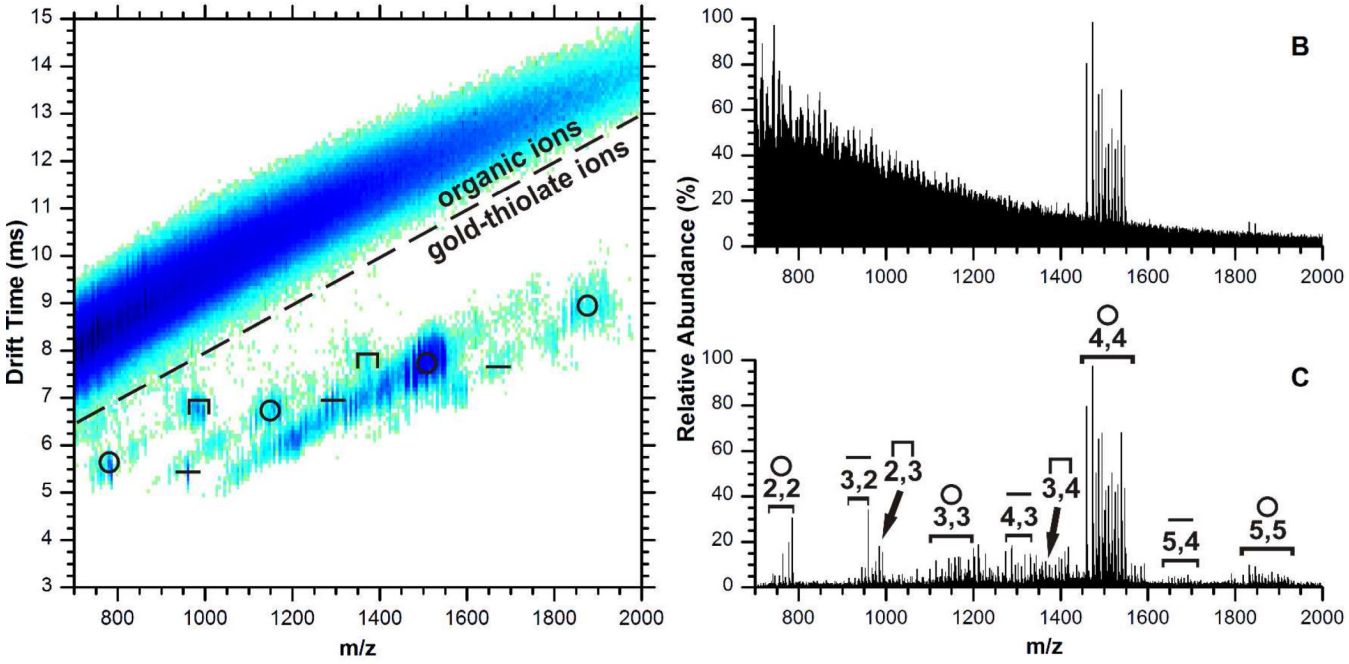

Figure 2.

Ion mobility-mass spectrum of tiopronin-protected AuNPs in positive ion mode (A), and the total (B) and extracted (C) mass spectrum. Extracted signal is from the outlined region of the two dimensional plot. The symbols above of the ion species in the IM-MS plot indicate their assigned structure as in Figure 1. In panel C, species are labeled by their molecular formula *x*,*y* for $Au_x(Tio)_y$.

NIH-PA Author Manuscript NIH-PA Author Manuscript NIH-PA Author Manuscript

NIH-PA Author Manuscript
NIH-PA Author Manuscript
NIH-PA Author Manuscript

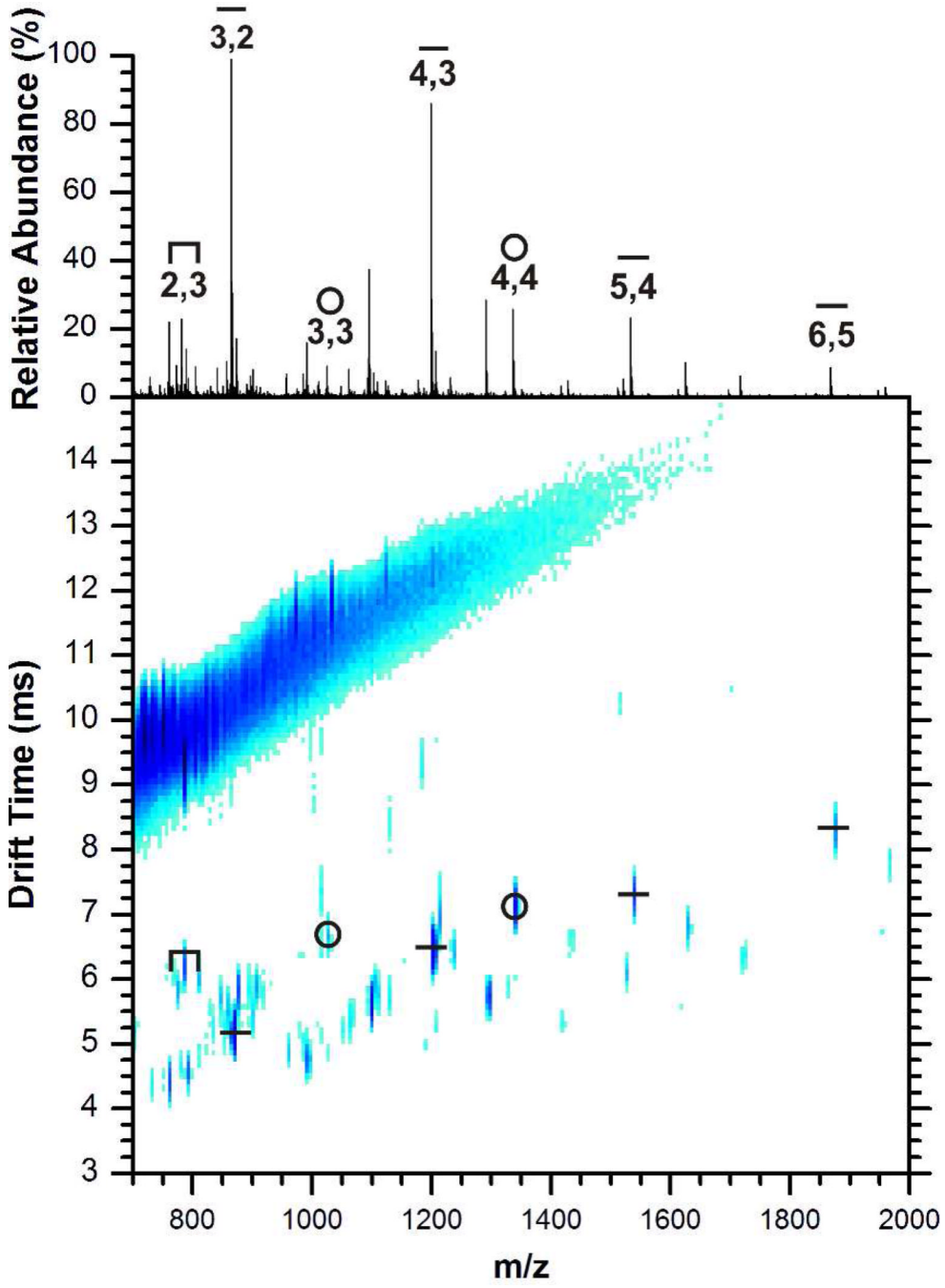

Figure 3.

Positive ion mobility-mass spectrum of phenylethanethiolate-protected AuNPs and the extracted mass spectrum (above). The highest intensity ions correspond to linear structures, but the tetrameric $[Au_4(SCH_2CH_2Ph)_4]^+$ is present, as well as the $Au_2(SCH_2CH_2Ph)_3$ staple species.

NIH-PA Author Manuscript
NIH-PA Author Manuscript
NIH-PA Author Manuscript

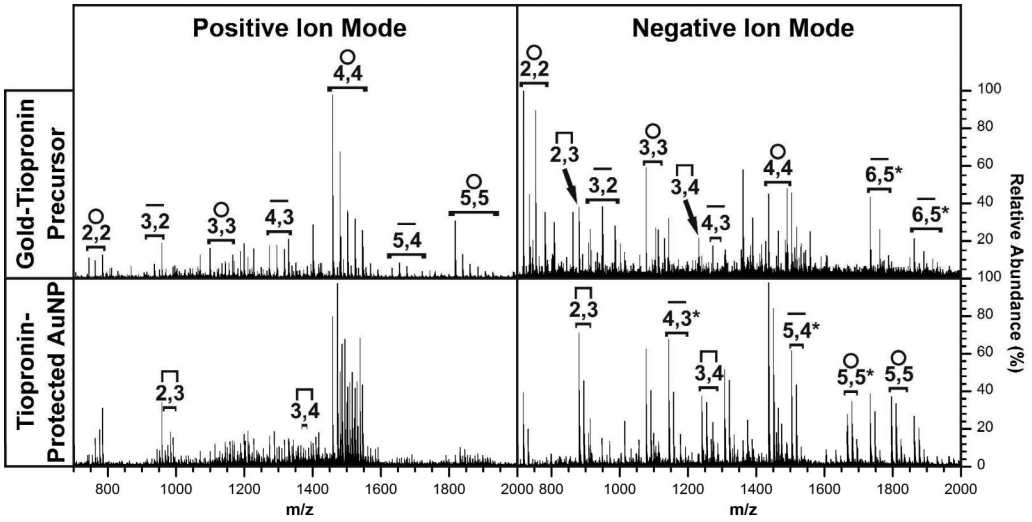

Figure 4.

Extracted mass spectra of gold-tiopronin precursor complexes (top) and tiopronin-protected AuNPs (bottom) in positive (left) and negative (right) ion mode. Structural assignment and stoichiometries are indicated as in previous figures. All assignments in above spectra are applicable to spectra underneath, with notable differences marked in the lower spectra.